ISSN 2616-5805 Vol. 6, Issue 1: 73-81, DOI: 10.25236/AJMS.2025.060109

Stability of vertically and extensible cantilevered pipes conveying fluid under the effects of different slenderness ratio and gravity

Yumei Luo[1], Yundong Li[1,2,*], Linyan Li[1], Zhongxiang Li[1]

[1]School of Mathematics and Statistics, Sichuan University of Science and Engineering, Zigong, 643000, China
[2]South Sichuan Center for Applied Mathematics, Sichuan University of Science and Engineering, Zigong, 643000, China
**Corresponding author: lyd1114@126.com*

Abstract: *Considering the influences of the rotational inertia and shear variables, the dynamical mathematical model for the vertically and extensible cantilevered pipes conveying fluid was established, and analyzed the stability of cantilevered pipes under different gravity and slenderness ratio. Based on the geometrically exact beam theory obtained the structural stiffness matrix of the cantilevered pipe, derived cantilevered pipes expression of the elastic potential energy. An extended Hamilton's principle was applied to establish a plane dynamic control equation for the cantilevered pipe, which includes the coupling between axial displacement, lateral displacement, and angular displacement. The weak form quadrature element method was used to discretize the dynamic control equation, then analyzed the variation under the different slender ratios and gravity by the numerical results.*

Keywords: *Cantilevered pipes; The geometrically exact beam theory; Gravity; Slenderness ratio*

1. Introduction

As an important structure for conveying fluid, the cantilevered pipes are extensively used in engineering fields [1]-[3]. In the practical application to enhance work efficiency, it is usually preferable to design the pipe with as high a critical flow velocity as possible. However, as a non-conservative system, the cantilevered pipes are prone to losing stability at high speeds. Thus, performing stability analysis of the cantilevered pipes is crucial not only for structural design and optimization but also for improving the operational efficiency and safety of the conveying system.

In recent years, there has been an increasing body of research discussing the stability analysis of cantilever flow pipe. Paidoussis [4]-[8] derived the dynamic equations for cantilevered pipes conveying fluid based on the Timoshenko beam theory and the Euler beam theory, and verified the correctness of the results by comparing with both theoretical and experimental data, thereby conducting an analysis of the stability of cantilevered pipes. Shayo [9]analyzed the stability of the cantilevered circular pipe with shaft movement under different slenderness ratios. Pramila A et al [10] analyzed vibration and stability of cantilevered pipes conveying fluid based the Timoshenko beam theory. Doaré et al [11] analyzed the effect of increasing length on the stability of a hanging fluid-conveying pipe is investigated. Texier et al [12] studied the deformation of an elastic pipe submitted to gravity and to an internal fluid flow by experiment. Huo et al [13] used Euler–Bernoulli beam theory and Hamilton's principle derived the differential equation of the pipe, studied the dynamical behavior of the system under the different flow velocity, instantaneous length of pipe, gravity, and mass ratio. Bai Y et al [14] established a dynamic model for cantilevered pipes conveying a variable density to analyze the influences of the fluctuating amplitude, wave number and initial phase angle of the fluid density on the stability and dynamics of the cantilevered pipe system. ElNajjar et al [15] derived the equation of motion of the system based on the linear theory of elasticity model assumption, analyzed the possibility of increasing the stability of the system by considering one or more additional masses and/or springs at various locations along the pipe. Chang X and Hong X [16] derived the dynamic equation for a cantilevered pipe conveying fluid with a nonlinear energy sink under pulsating flow, and investigated the stability of cantilevered fluid-conveying pipe. Mi L D et al [17] based on the stable slug flow model and hysteretic model to study the dynamics and stability of a cantilevered piping system conveying slug flow. Previous research has shown that many scholars have nearly all established the dynamical models of cantilever pipes conveying fluid based on the Timoshenko beam

ISSN 2616-5805 Vol. 6, Issue 1: 73-81, DOI: 10.25236/AJMS.2025.060109

theory[18] and Euler-Bernoulli beam theory[19], and then analyzed various factors affecting the system stability. However, the dynamical behavior of cantilevered pipes is more complex and variable in practical engineering applications. Therefore, establishing a more accurate dynamical model is of great significance for ensuring the reliability of the structural and the stability of the system.

Timoshenko beam theory and Euler-Bernoulli beam theory are theories based on the assumption of small deformations and linear elasticity. Geometrically exact beam theory [20]-[26] account for the influence of non-linear structural changes, using strain fields, stress fields, and deformation variations to more accurately describe and predict the mechanical behavior of structures under large strains and large displacements. More importantly, the strain proposed by geometrically exact beam theories is objective, which provides a unified measurement standard for structural analysis to fully reflecting the deformation conditions of the cross-section of the structure. Compared with traditional beam theories, geometrically exact beam theories are a more efficient and accurate mechanical theory to describe the mechanical behavior of structures.

This study considering the effects of rotational inertia and shear deformation, based on the geometrically exact beam theory and the extended Hamiltonian principle to found the dynamical mathematical model for the vertically and extensible cantilevered pipes conveying fluid. The weak form quadrature element method [27]-[28] is applied for the discrete solution of the governing equations, and the correctness of the theoretical analysis is verified through numerical simulation results. Moreover, this paper analyzed the effect of the slenderness ratio and gravity on the stability of cantilevered pipes system.

2. Found the dynamical model

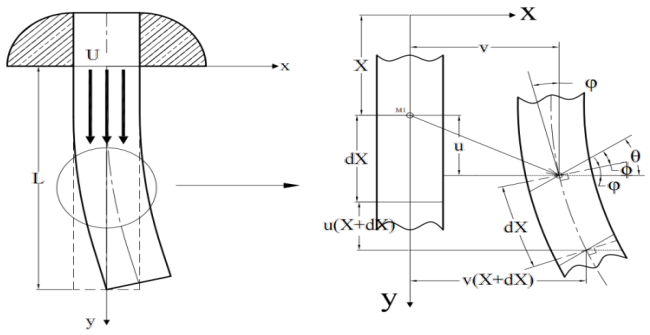

Figure 1 The pipe schematic diagram.

The system under consideration consists of the pipe of length L, cross-sectional area A_p, the outer diameter of the pipe is D_p, cross-sectional moment of inertia I_p, Young's modulus E, Poisson ratio ν, density ρ_p, and mass per unit length m_p, conveying fluid of density ρ_f, cross-sectional area A_f, the inner diameter is D_f, and mass per unit length m_f, with flow velocity U. Moreover, in this paper, $(\,)'$ represents the first-order derivative with respect to X, $(\,)''$ represents the second-order derivative with respect to X, $\bullet$ denotes the first-order derivative with respect to time, $\bullet\bullet$ denotes the second - order derivative with respect to time. In the Figure 1, ϕ is the shear deformation angle, φ is the rotational angle of the neutral axis, and θ is the rotational angle of the cross-section, where $\theta = \phi + \varphi$.

Lagrange description is mainly used to describe the motion and deformation of solid materials in structural analysis, so the initial configuration of the pipeline is selected as the reference. Axial displacement u and transverse displacement v are introduced to describe the displacement of any point on the pipe axis after deformation, and the θ represents the rotation angle of the cross section where the particle is located to describe the rotation of the cross section where the point is located after deformation. Where u, v and θ are all functions of X. Therefore, the configuration of the pipe can be fully represented by the following displacement vector

$$\varsigma = (u, v, \theta)^T \tag{1}$$

ISSN 2616-5805 Vol. 6, Issue 1: 73-81, DOI: 10.25236/AJMS.2025.060109

For convenience of derivation, let $\boldsymbol{\lambda}_1 = \left(cos\theta \quad sin\theta\right)^T$ which is perpendicular the cross-section, and let $\boldsymbol{\lambda}_2 = \left(-sin\theta \quad cos\theta\right)^T$ which is parallel to the cross-section.

Assuming that in the initial state, the initial position of a point on the pipe is $\mathbf{X}\left(X,Y\right)^T$, and $\mathbf{x}\left(x,y\right)^T$ is the location of the point after deformation in the current configuration. Based on the assumption of the plane section, the following can be obtained

$$\mathbf{x} = (x,y)^T, \quad \mathbf{r} = \left(X+u,v\right)^T \tag{2}$$

where $\mathbf{r}$ is the centroid position of the current cross-section.

Considering the local rotation of the neutral axis denoted φ, one obtains

$$\sin\varphi = v'/1+e, \quad \cos\varphi = \left(1+u'\right)/1+e \tag{3}$$

where is the strain along the neutral axis of the pipe.

The Ressiner strain vector based on the geometrically exact beam theory is

$$\boldsymbol{\chi} = \left[\varepsilon \quad \gamma \quad \kappa\right]^T = \left[\boldsymbol{\lambda}_1^T\mathbf{r}' - 1 \quad \boldsymbol{\lambda}_2^T\mathbf{r}' \quad \theta'\right]^T \tag{4}$$

where ε is axial strain, γ is shear strain, and κ is bending strain of the pipe.

The velocity of the pipe at the center axis is

$$\mathbf{v}_p = \dot{\mathbf{r}} = \dot{u}\mathbf{i}_x + \dot{v}\mathbf{i}_y \tag{5}$$

where $\mathbf{i}_x$ and $\mathbf{i}_y$ are unit vectors.

The kinetic energy of the pipe

$$T_p = \frac{1}{2}m_p\int_0^L \dot{u}^2 + \dot{v}^2 ds + \frac{1}{2}I_p\int_0^L \dot{\theta}^2 ds \tag{6}$$

The velocity of the fluid is

$$\mathbf{v}_F = \mathbf{v}_P + U\left(1-ae\right)\mathbf{r}' \tag{7}$$

where $a = 1-2\nu$ [8], $\mathbf{r}'$ is the direction vector tangent to the centerline of the pipe.

The kinetic energy of the fluid is

$$T_f = \frac{1}{2}m_f\int_0^L \begin{bmatrix} \dot{u}^2 + U^2 + 2U^2u' + U^2u'^2 - 2aU^2u' + 2U\dot{u} + 2U\dot{u}u' \\ \dot{v}^2 + 2U\dot{v}v' - aU^2v'^2 + U^2v'^2 \end{bmatrix} dX \tag{8}$$

The potential energy of the pipe includes elastic potential energy and gravitational potential energy, which are respectively expressed as follows

$$V_P = \frac{1}{2}\int_0^L \boldsymbol{\chi}^T D\boldsymbol{\chi} dX \tag{9}$$

$$V_g = -\left(m_P + m_F\right)\left(g \quad 0\right)^T \int_0^L \mathbf{r} dX \tag{10}$$

where g is the gravitational coefficient, and D is the material constitution relation matrix.

$$D = \begin{bmatrix} EA & 0 & 0 \\ 0 & k_S GA & 0 \\ 0 & 0 & EI \end{bmatrix} \tag{11}$$

where k_s is shear correction factor.

ISSN 2616-5805 Vol. 6, Issue 1: 73-81, DOI: 10.25236/AJMS.2025.060109

The virtual work done by non-conservative forces in the pipe system is

$$\delta\int_{t1}^{t2} Wdt = \int_{t1}^{t2} m_f U\left(\dot{\mathbf{r}}_L + U\mathbf{r}_L'\right)\delta\mathbf{r}_L dt \tag{12}$$

where $\mathbf{r}_L$ and $\mathbf{r}_L'$ respectively represent the position vector and tangent vector of the centroid of the pipe at the terminal cross-section.

As the cantilever pipeline system is a non-conservative system, the dynamic equations of the system are obtained based on the extended Hamilton's principle

$$\delta\int_{t1}^{t2}\left(T-V\right)dt - \delta\int_{t1}^{t2} Wdt = 0 \tag{13}$$

Based on the Hamilton's variational principle, the times $t1$ and $t2$ are fixed, thus the variation $\delta u\big|_{t_1}=0$, $\delta u\big|_{t_2}=0$ 1, $\delta v\big|_{t_1}=0$、, $\delta v\big|_{t_2}=0$, $\delta\theta\big|_{t_1}=0$, $\delta\theta\big|_{t_2}=0$. Moreover, since $\delta u,\delta v,\delta\theta$ are respectively independent variations to ensure equation (13) hold, thus $\delta\left(T-V-W\right)=0$, thereby yielding the vibration model of the pipeline as follows

$$\begin{aligned}&\int_0^L\left(m_p+m_f\right)\ddot{u}\delta u dX + \int_0^L\left(m_p+m_f\right)\ddot{v}\delta v dX + \rho_p I_P\int_0^L\ddot{\theta}\delta\theta dX\\ &+am_f U^2\int_0^L\left(\delta u'+v'\delta v'\right)dX + m_f U^2\int_0^L\left[u''\delta u+v''\delta v\right]dX\\ &+2m_f U\int_0^L\left(\dot{u}'\delta u+\dot{v}'\delta v\right)dX + \int_0^L\delta\chi^T D\chi dX - \left(m_p+m_f\right)g\int_0^L\left(\delta X+\delta u\right)dX = 0\end{aligned} \tag{14}$$

where $\delta\boldsymbol{\chi}$ is expressed as follows

$$\delta\boldsymbol{\chi} = \boldsymbol{\Gamma}\begin{Bmatrix}\delta\varsigma'\\ \delta\theta\end{Bmatrix} = \begin{bmatrix}\boldsymbol{\lambda}_1^T & 0 & \boldsymbol{\lambda}_2^T\mathbf{r}'\\ \boldsymbol{\lambda}_2^T & 0 & -\boldsymbol{\lambda}_1^T\mathbf{r}'\\ 0_{1\times2} & 1 & 0\end{bmatrix}\begin{Bmatrix}\delta\mathbf{r}'\\ \delta\theta'\\ \delta\theta\end{Bmatrix} \tag{15}$$

Define the node displacement vector of the pipe:

$$\mathbf{d} = \begin{bmatrix}\varsigma_1^T & \cdots & \varsigma_k^T & \cdots & \varsigma_N^T\end{bmatrix}^T,\ k=1,\cdots,N \tag{16}$$

Using the differential quadrature principle from Ref [29] and equation (15), we obtain $\delta\boldsymbol{\chi}_k$ represented by $\delta\mathbf{d}$

$$\delta\boldsymbol{\chi}_k = \boldsymbol{\Gamma}_k\begin{Bmatrix}\delta\varsigma_k'\\ \delta\beta_k\end{Bmatrix} = \boldsymbol{\Gamma}_k\mathbf{B}_k\delta\mathbf{d} \tag{17}$$

where $\delta\zeta_k = \mathbf{A}_k\delta\mathbf{d}, \mathbf{A}_k = \begin{bmatrix}\delta_{k1}\mathbf{I}_{3\times3} & \cdots & \delta_{ki}\mathbf{I}_{3\times3} & \cdots & \delta_{kn}\mathbf{I}_{3\times3}\end{bmatrix}$, $\mathbf{I}$ is identity matrix.

The differential quadrature positioning matrix can be expressed as :

$$\mathbf{B}_k = \begin{bmatrix}\mathbf{b}_{k1} & \cdots & \mathbf{b}_{ki} & \cdots & \mathbf{b}_{kn}\end{bmatrix} \tag{18}$$

where $\mathbf{b}_{ki} = \begin{bmatrix}\frac{2}{L^e}C_{ki}^{(1)}\mathbf{I}_{3\times3}\\ \boldsymbol{\alpha}_{ki}\end{bmatrix}$, $\boldsymbol{\alpha}_{ki} = \left(0,0,\delta_{ki}\right)$, $\delta_{ki} = \begin{cases}1, k=i\\ 0, k\neq i\end{cases}$ from Ref [28].

Introducing dimensionless parameters

$$\xi = \frac{2}{L}X - 1,\quad \xi\in\left[-1,1\right] \tag{19}$$

Based on the weak form quadrature method [27]-[28], the weak form vibration equation of the pipe is

$$\mathbf{M}\ddot{\mathbf{d}} + \mathbf{C}f\dot{\mathbf{d}} + \mathbf{K}_u\mathbf{d} + \mathbf{K}_T\mathbf{d} + \mathbf{G} + \mathbf{C} = \mathbf{0} \tag{20}$$

ISSN 2616-5805 Vol. 6, Issue 1: 73-81, DOI: 10.25236/AJMS.2025.060109

where the mass matrix of the pipe is

$$\mathbf{M}=\frac{L}{2}\sum_{k=1}^{N}w_k\left[\left(\rho_p A_p+\rho_f A_f\right)\left(\mathbf{E1}_k{}^T\mathbf{E1}_k+\mathbf{E2}_k{}^T\mathbf{E2}_k\right)+\rho_p I_p\mathbf{E3}_k{}^T\mathbf{E3}_k\right] \tag{21}$$

where $\mathbf{E1}$ represents an $N\times 3N$ matrix where the element in the k-th row and the 3k-2-th column is 1, and all other elements are 0, and $\mathbf{E1}_k$ represents the k-th row of $\mathbf{E1}$. $\mathbf{E2}$ represents $N\times 3N$ matrix where the element in the k-th row and the 3k-1)-th column is 1, and all other elements are 0, and $\mathbf{E2}_k$ represents the k-th row of $\mathbf{E2}$. $\mathbf{E3}$ represents an $N\times 3N$ matrix where the element in the k-th row and the 3k-th column is 1, and all other elements are 0, and $\mathbf{E3}_k$ represents the k-th row of $\mathbf{E3}$.

$$\mathbf{Cf}=2\rho_f A_f U\sum_{k=1}^{N}w_k\left(\mathbf{E1}_k^T\sum_{j=1}^{N}C_{kj}^{(1)}\mathbf{E1}+\mathbf{E2}_k^T\sum_{j=1}^{N}C_{kj}^{(1)}\mathbf{E2}\right) \tag{22}$$

$$\mathbf{G}=-\frac{L}{2}\left(\rho_p A_p+\rho_f A_f\right)g\sum_{k=1}^{N}w_k\mathbf{E1}_k{}^T \tag{23}$$

$$\mathbf{C}=a\rho_f A_f U^2\sum_{k=1}^{N}w_k\mathbf{E1}^T\sum_{j=1}^{N}C_{kj}^{(1)T} \tag{24}$$

$$\mathbf{K}_u=\frac{2}{L}\rho_f A_f U^2\sum_{k=1}^{N}w_k\left(a\mathbf{E2}^T\sum_{j=1}^{N}C_{kj}^{(1)T}\sum_{j=1}^{N}C_{kj}^{(1)}\mathbf{E}2+\mathbf{E1}_k^T\sum_{j=1}^{N}C_{kj}^{(2)}\mathbf{E1}+\mathbf{E2}_k^T\sum_{j=1}^{N}C_{kj}^{(2)}\mathbf{E}2\right) \tag{25}$$

The tangential stiffness matrix of the element as follows

$$\mathbf{K}_T=\frac{L}{2}\sum_{k=1}^{n}w_k\mathbf{B}_k^T\left(\mathbf{\Gamma}_k^T\mathbf{D}_k\mathbf{\Gamma}_k+\mathbf{\Xi}_k\right)\mathbf{B}_k \tag{26}$$

where $\mathbf{\Xi}_k$ is expressed as follows

$$\mathbf{\Xi}_k=\begin{bmatrix}\mathbf{0}_{2\times 2} & \mathbf{0}_{2\times 1} & -k_s GA\gamma_k\boldsymbol{\lambda}_{1k}+EA\varepsilon_k\boldsymbol{\lambda}_{2k}\\ \mathbf{0}_{1\times 2} & 0 & 0\\ -k_s GA\gamma_k\boldsymbol{\lambda}_{1k}^T+EA\varepsilon_k\boldsymbol{\lambda}_{2k}^T & 0 & -EA\varepsilon_k\boldsymbol{\lambda}_{1k}^T\boldsymbol{r}_k'-k_s GA\gamma_k\boldsymbol{\lambda}_{2k}^T\boldsymbol{r}_k'\end{bmatrix} \tag{27}$$

From equation (26), the stiffness matrix of the structure is from $\mathbf{K}_T$ when $\mathbf{d}=0$.

Let $d=d^*+d_s$, thus

$$\mathbf{M}\left(\ddot{\mathbf{d}}^*+\ddot{\mathbf{d}}_s\right)+\mathbf{Cf}\left(\dot{\mathbf{d}}^*+\dot{\mathbf{d}}_s\right)+\mathbf{K}_u\left(\mathbf{d}^*+\mathbf{d}_s\right)+\mathrm{K}_T\left(\mathbf{d}^*+\mathbf{d}_s\right)=-\left(G+C\right) \tag{28}$$

then combine the equation (20) with equation (28) to linearize the equation

$$\mathbf{M}\ddot{\mathbf{d}}+\mathbf{Cf}\dot{\mathbf{d}}+\left(\mathbf{K}_u+\mathbf{K}_T\right)\mathbf{d}=\mathbf{0} \tag{29}$$

Let $\dot{\mathbf{q}}_1=\mathbf{q}_2=\dot{\mathbf{d}}$, $\dot{\mathbf{q}}_2=\ddot{\mathbf{q}}_1=\ddot{\mathbf{d}}$, thus the natural frequency can be obtained by solving the state equation as follows

$$\begin{aligned}&\mathbf{M}\dot{\mathbf{q}}_2+\mathbf{Cf}\mathbf{q}_2+\left(\mathbf{K}_u+\mathbf{K}_T\right)\mathbf{q}_1=\mathbf{0}\\ &\begin{bmatrix}\dot{\mathbf{q}}_1\\ \dot{\mathbf{q}}_2\end{bmatrix}=\begin{bmatrix}\mathbf{0} & \mathbf{E}\\ \left(\mathbf{K}_u+\mathbf{K}_T\right)\left(-\mathbf{M}^{-1}\right) & \mathbf{Cf}_1\end{bmatrix}\begin{bmatrix}\mathbf{q}_1\\ \mathbf{q}_2\end{bmatrix}\end{aligned} \tag{30}$$

The dimensional parameter is as follows

ISSN 2616-5805 Vol. 6, Issue 1: 73-81, DOI: 10.25236/AJMS.2025.060109

$$U_f = \sqrt{\frac{m_f}{EI}}UL,\ \beta = \frac{m_f}{m_p + m_f},\ \gamma_g = \left(m_p + m_f\right)g\frac{L^3}{EI},\ \omega_\xi = \omega L^2\sqrt{\frac{m_p + m_f}{EI}} \tag{31}$$

where U_f is the dimensionless velocity, β is the mass ratio coefficient, γ_g is the gravity term coefficient, and ω_ξ is the dimensionless frequency.

3. Numerical results and discussion

For improving the accuracy of numerical calculation results, in this paper uses two units for numerical calculation, each unit contains 11 nodes. The parameters of the pipe are respectively $E = 210Gpa$, $D_p = 0.1885m$, $D_f = 0.1825m$, $\rho_p = 7850kg/m^3$, $\rho_p = 1000kg/m^3$, $\nu = 0.3$.

By comparing the numerical results in Table 1, it can be found that the maximum relative error between the numerical results obtained and those in reference[30] is less than 0.50%. Furthermore, the results in the Figure 2 are also similar to the results found in reference[4] and reference[11].This not only proves the correctness of the model, but also demonstrated the efficiency of the model, which can ensure the calculation accuracy while selecting fewer parameters.

Table 1 Natural frequency of pipes at u=0.

	Ref[30]	Ref[31]	Present work	Error %
w_1	3.5160	3.5160	3.5154	0.17
w_2	22.0345	22.0345	22.0097	0.11
w_3	61.6972	61.6972	61.5322	0.27
w_4	120.9019	120.9019	120.3064	0.49

When the real part of the vibration equation's eigenvalue is greater than zero, the pipe will exhibit flutter instability. The speed corresponding to the instability point is the critical flow velocity U_{cr}. $L_r = L/r$ is the slenderness ratio, where $r = \sqrt{I/\left(A_p - A_f\right)}$ is the moment of inertia radius of. In the Figure 2, $U_{Vcr} = U_f\gamma_g^{-1/3}$, and $L_\gamma = \gamma_g^{1/3}$, and shows that for pipes of fixed length, an increase in gravity can enhance pipeline stability.

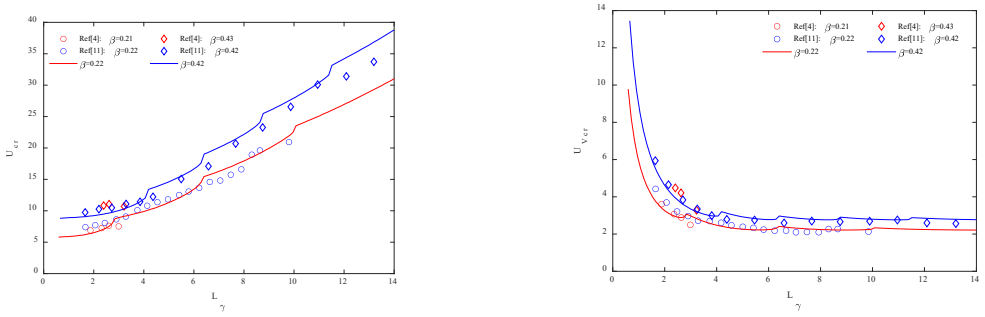

Figure 2 (a) Dimensionless velocity based on the pipe length, (b) Dimensionless velocity based on gravity

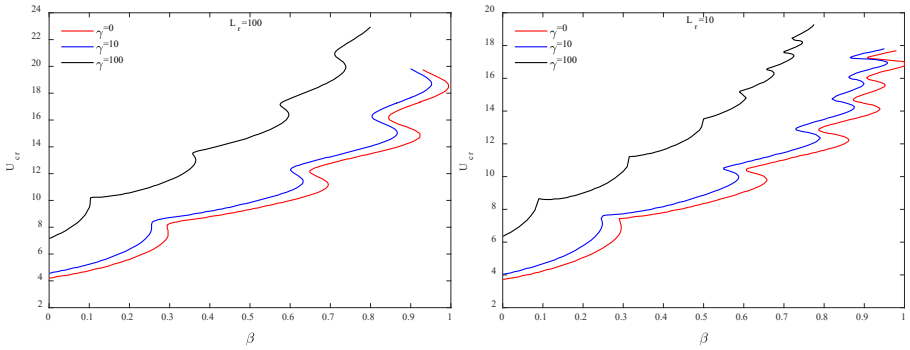

Figure 3 Gravity effects on U_{cr} for the cantilevered pipe, (a), $L_r = 100$, (b), $L_r = 10$.

ISSN 2616-5805 Vol. 6, Issue 1: 73-81, DOI: 10.25236/AJMS.2025.060109

In the figure 3, S-shaped curves occur because the cantilevered pipe is significantly influenced by the slenderness ratio, such that under a single mass ratio coefficient, multiple critical flow velocities can correspond. Taking into account the variation of the critical flow velocity with different gravity coefficients when the slenderness ratio $L_r = 100$, and $L_r = 10$ to study the effects of gravity on the system stability of long pipes and short pipes. The data from Figure 3 (a) is agreed with the results from reference[4]. Moreover, it can be observed from Figure 3, the critical velocity increases with the increase of gravity when the same value of β and L_r, and the critical velocity also increases with the gravitational ratio coefficient increase of when the same value of L_r and γ_g.

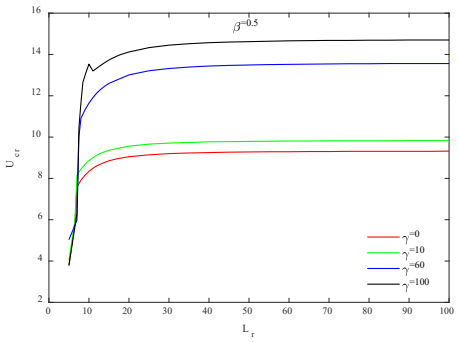

Figure 4 Slenderness ratio effects on U_{cr} for cantilevered pipes

In the Figure 4, it shows that the variation of the critical flow velocity with the slenderness ratio under the different gravity when $\beta = 0.5$. It can be found that the change in gravity significantly affects the influence of slenderness ratio on the critical flow velocity. Under the same gravity, the critical flow velocity increases with the increase of the slenderness ratio, when the slenderness ratio exceeds 100, at which point the critical flow velocity tends to stabilize.

The numerical results of Table 2 show the variation of the critical velocity of the system with the value of a, gravity term coefficient and mass ratio coefficients. The critical velocity of the system increases with the increase of a when the same value of β and γ. The critical velocity of the system increases with the increase of γ when the same value of β and a.

Table 2 The critical flow velocity under different values of a, γ.

		a=0.12					a=0.4		
		γ=0	γ=0		γ=10	γ=100	γ=0	γ=10	γ=100
	β	Ref[8]	Present work	Error (%)	Present work	Present work	Present work	Present work	Present work
U_{cr}	0.145	5.1226	5.08	0.84	5.65	10.29	5.09	5.66	10.3
	0.250	6.2928	6.22	1.17	7.48	10.96	6.23	7.49	10.96
	0.470	9.1558	9.14	0.17	9.62	14.42	9.15	9.63	14.43

4. Conclusions

In this study, the effects of slenderness ratio and gravity on the stability of the extensible cantilevered pipe is investigated. By comparing the numerical simulation results with reference data, the correctness of the plane dynamics mathematical model of the cantilever pipe established based on the geometrically exact beam theory was verified. The following conclusions on the influence of gravity and slenderness ratio on the stability of the vertical cantilever pipe can be drawn from the results of this study:

(1) For the same slenderness ratio and gravity ratio coefficients, an increase in gravity can enhance the stability of the system of cantilevered pipes conveying fluid.

(2) For the same influence of gravity, an increase in the slenderness ratio can improve the stability of the system of cantilevered pipes conveying fluid.

(3) For systems of cantilevered pipes conveying fluid, an increase in the gravity parameter and the mass ratio coefficient leads to a greater number of S-shaped curves.

ISSN 2616-5805 Vol. 6, Issue 1: 73-81, DOI: 10.25236/AJMS.2025.060109

(4) For the same conditions, the critical flow velocity of cantilevered pipes increasing with the increase of the value of a, and appropriately considering the a can enhance the stability of the system.

References

[1] Harija H, George B, Tangirala A K. A cantilever-based flow sensor for domestic and agricultural water supply system[J]. IEEE Sensors Journal, 2021, 21(23): 27147-27156.

[2] Shen X, Feng K, Xu H, et al. Reliability analysis of bending fatigue life of hydraulic pipeline[J]. Reliability Engineering & System Safety, 2023, 231: 109019.

[3] Yang S, Gao H, Wu Q. Vibration Characteristics and Frequency Modulation of Rocket Engine Multiconfiguration Small Pipeline Systems[J]. AIAA Journal, 2024, 62(12): 4812-4823.

[4] Paidoussis M P. Dynamics of tubular cantilevers conveying fluid[J]. Journal of Mechanical Engineering Science, 1970, 12(2): 85-103.

[5] Paidoussis M P, Issid N T. Dynamic stability of pipes conveying fluid[J]. Journal of sound and vibration, 1974, 33(3): 267-294.

[6] Paıdoussis M P, Laithier B E. Dynamics of Timoshenko beams conveying fluid [J][J]. Journal of Mechanical Engineering Science, 1976, 18(2): 210-220.

[7] Paidoussis M P, Luu T P, Laithier B E. Dynamics of finite-length tubular beams conveying fluid[J]. Journal of Sound and Vibration, 1986, 106(2): 311-331.

[8] Ghayesh M H, Païdoussis M P, Amabili M. Nonlinear dynamics of cantilevered extensible pipes conveying fluid[J]. Journal of Sound and Vibration, 2013, 332(24): 6405-6418.

[9] Shayo L K, Ellen C H. Theoretical studies of internal flow-induced instabilities of cantilever pipes[J]. Journal of sound and vibration, 1978, 56(4): 463-474.

[10] Pramila A, Laukkanen J, Liukkonen S. Dynamics and stability of short fluid-conveying Timoshenko element pipes[J]. Journal of Sound and Vibration, 1991, 144(3): 421-425.

[11] Doaré O, de Langre E. The flow-induced instability of long hanging pipes[J]. European Journal of Mechanics-A/Solids, 2002, 21(5): 857-867.

[12] Texier B D, Dorbolo S. Deformations of an elastic pipe submitted to gravity and internal fluid flow[J]. Journal of Fluids and Structures, 2015, 55: 364-371.

[13] Huo Y, Wang Z. Dynamic analysis of a vertically deploying/retracting cantilevered pipe conveying fluid[J]. Journal of Sound and Vibration, 2016, 360: 224-238.

[14] Bai Y, Xie W, Gao X, et al. Dynamic analysis of a cantilevered pipe conveying fluid with density variation[J]. Journal of Fluids and Structures, 2018, 81: 638-655.

[15] ElNajjar J, Daneshmand F. Stability of horizontal and vertical pipes conveying fluid under the effects of additional point masses and springs[J]. Ocean Engineering, 2020, 206: 106943.

[16] Chang X, Hong X. Stability and nonlinear vibration characteristics of cantilevered fluid-conveying pipe with nonlinear energy sink[J]. Thin-Walled Structures, 2024: 111987.

[17] Mi L D, Zhou Y L, Yang M. Dynamic stability of cantilevered piping system conveying slug flow[J]. Ocean Engineering, 2023, 271: 113675.

[18] Timoshenko S P. LXVI. On the correction for shear of the differential equation for transverse vibrations of prismatic bars[J]. The London, Edinburgh, and Dublin Philosophical Magazine and Journal of Science, 1921, 41(245): 744-746.

[19] Bauchau O A, Craig J I. Euler-Bernoulli beam theory[M]//Structural analysis. Dordrecht: Springer Netherlands, 2009: 173-221.

[20] Reissner E. On one-dimensional finite-strain beam theory: the plane problem[J]. Zeitschrift fur angewandte Mathematik und Physik ZAMP, 1972, 23(5): 795-804.

[21] Reissner E. On one-dimensional large displacement finite-strain beam theory[J]. Studies in applied mathematics, 1973, 52(2): 87-95.

[22] Reissner E. On finite deformations of space-curved beams[J]. Zeitschrift fur angewandte Mathematik und Physik ZAMP, 1981, 32(6): 734-744.

[23] Simo J C. A finite strain beam formulation. The three-dimensional dynamic problem. Part I[J]. Computer methods in applied mechanics and engineering, 1985, 49(1): 55-70.

[24] Simo J C, Vu-Quoc L. A three-dimensional finite-strain rod model. Part II: Computational aspects[J]. Computer methods in applied mechanics and engineering, 1986, 58(1): 79-116. 1986; 58(1): 79-116.

[25] Simo J C, Vu-Quoc L. A geometrically-exact rod model incorporating shear and torsion-warping deformation[J]. International Journal of Solids and Structures, 1991, 27(3): 371-393.

[26] Vu-Quoc L, Li S. Dynamics of sliding geometrically-exact beams: large angle maneuver and parametric resonance[J]. Computer methods in applied mechanics and engineering, 1995, 120(1-2): 65-118.

ISSN 2616-5805 Vol. 6, Issue 1: 73-81, DOI: 10.25236/AJMS.2025.060109

[27] Zhong H, Yu T. Flexural vibration analysis of an eccentric annular Mindlin plate[J]. Archive of Applied Mechanics, 2007, 77: 185-195.
[28] Xiao N, Zhong H. Non-linear quadrature element analysis of planar frames based on geometrically exact beam theory[J]. International Journal of Non-Linear Mechanics, 2012, 47(5): 481-488.
[29] Bellman R, Casti J. Differential quadrature and long-term integration[J]. Journal of mathematical analysis and Applications, 1971, 34(2): 235-238.
[30] Ni Q, Zhang Z L, Wang L. Application of the differential transformation method to vibration analysis of pipes conveying fluid[J]. Applied Mathematics and Computation, 2011, 217(16): 7028-7038.
[31] William T T. THEORY OF VIBRATION WITH APPLICATIONS[M]. Prentice-Hall, Incorporated, 1988.